ISSN: 2756-2638
Transactions on Engineering and Computing Sciences; Vol. 14 No. 04 (2026) (20-37)
https://doi.org/10.14738/tmlai.1404.11963

Frequency-Domain Characterization of Fractional Variable-Order Systems with Scarpi Derivatives

Trupti V. Mahajan, Mukesh D. Patil, Vishwesh A. Vyawahare

Department of Electronics Engineering, Ramrao Adik Institute of Technology, Dr. D Y Patil Vidyanagar, Navi Mumbai, India 400706

Abstract: This work presents a frequency-domain analysis framework for fractional variable-order (FVO) linear systems using the Scarpi derivative approach. Unlike classical fractional-order models with fixed differentiation orders, variable-order systems give greater flexibility to more accurately model a more dynamic system whose memory effects change over time or depending on certain operating conditions. The Scarpi derivative is a consistent mathematical way to preserve the necessary properties for analyzing variable-order dynamics and deriving frequency-domain transfer function representations. A generalized frequency response is created, which represents a linear system modeled using Scarpi (variable-order) operators, then examined the impacts on the magnitude and phase characteristics of the system caused by order variability. Here, methodology generalizes traditional Bode analyses into a variable-order fractional model. Additionally, the methodology illustrates how order variability affects the resonant behavior, bandwidth, stability margins, and robustness of the system. Numerical analysis also illustrated with an example to a complex system with time-varying memory effects. The results of this research indicate that using the Scarpi derivative formulation is an effective means of modeling and characterizing frequency-domain complex systems with nonstationary memory effects. This work has numerous potential applications in control engineering, viscoelastic materials, electrochemical processes, and living systems. The results contribute to the advancement of variable-order fractional calculus by establishing a practical and systematic framework for the frequency analysis of FVO linear systems.

Keywords: Linear Systems, Fractional-order systems, Variable-order calculus, Scarpi variable-order derivatives, Frequency-domain analysis.

INTRODUCTION

The linear control systems are widely used in engineering because they are easier to analyze, design, and implement than nonlinear systems. Its behavior can be described using linear differential equations. Linear control systems include simple mathematical modelling, predictable behaviour, and the availability of powerful analysis techniques such as transfer functions, frequency response, and state-space methods. Linear models are usually valid only within a specific operating range. Because of their simplicity and effectiveness, linear control systems remain a fundamental topic in electrical, mechanical, aerospace, and industrial engineering. Frequency-domain analysis is a method of studying how a linear control system responds to sinusoidal inputs of different frequencies. Instead of analyzing the system's behavior over time (time-domain analysis), it examines the relationship between input and output in terms of frequency, magnitude, and phase shift. For a linear time-invariant (LTI) system, the transfer function G(s) is evaluated by replacing s with $j\omega$.

Fractional calculus is a branch of mathematics that extends the concepts of differentiation and integration to non-integer (fractional) orders. While classical calculus deals with derivatives and integrals of integer order (first derivative, second derivative, etc.), fractional calculus allows operations such as half-order, quarter-order, or even irrational-order derivatives and integrals. fractional calculus is a powerful mathematical tool that generalizes classical calculus and enables more realistic modeling of systems with memory and complex dynamics. Fractional-order systems are particularly useful for modeling real-world processes that exhibit memory, hereditary effects, and long-term dependencies. In such systems, the current output depends not only on the present input but also on the past history of the system. This characteristic enables more accurate representation of many physical and engineering phenomena. The applications of fractional calculus (FC) also extend to other domains such as control systems, signal and image processing, Network analysis, artificial neural networks, machine learning, and for more details, refer to [1-10]. Recent years have witnessed the extension of FC to more advanced and complex derivatives such as complex-order derivatives, conjugated complex-order derivatives. Extensive work is done for fractional-order linear systems given in [11-13]. Frequency response analysis is an important technique for studying the dynamic behavior and stability of fractional-order linear control systems also analyzes system performance and handles sinusoidal inputs easily. It is used in electrical, mechanical, aerospace, and industrial control engineering. The frequency response of a system is obtained by substituting: (s = $j\omega$) where (ω) is the angular frequency, resulting in a transfer function whose magnitude and phase vary continuously with frequency. For a fractional-order element $G(s) = s^{\alpha}$, the frequency response becomes: $G(j\omega) = (j\omega)^{\alpha}$ which can be expressed as: $G(j\omega) = \omega^{\alpha} e^{j\alpha\pi/2}$ From this expression: Magnitude: $|G(j\omega)| = \omega^{\alpha}$ and phase: $\angle G(j\omega) = \alpha \times 90^{\circ}$ This result shows that a fractional-order element produces a constant phase shift proportional to its order (α). Consequently, the magnitude slope in a Bode plot is: 20α dB/decade rather than the integer multiples of 20 dB/decade found in conventional systems. This analysis provides valuable information about system stability, robustness, bandwidth, and resonance characteristics.

Podlubny discussed time domain analytical solutions of fractional differential equations, but it is very difficult to analyze as the expression with infinite terms does not converge in steady state and realization is complicated [1, 5]. A more convenient method is to analyze such systems properties in complex and frequency domain and finding the relationship of frequency properties between fractional-order systems and integer-order systems. Several steps explained in [14] for fractional-order systems transfer functions from frequency response diagrams, which expanded the range of identifiable systems. Fractional-order models and controllers have infinite dimensions. Therefore, their frequency responses cannot be implemented directly in the real world. Some applications are discussed in [4, 6, 25,26] also some chaos discussed in [20]. Bode plots are widely used for frequency response analysis of fractional-order systems. They consist of magnitude plot (gain versus frequency) and phase plot (phase angle versus frequency) For a fractional-order differentiator (s^{α}): Magnitude increases at (20α) dB/decade and phase remain constant at ($90\alpha^{\circ}$). For a fractional-order integrator ($1/s^{\alpha}$), magnitude decreases at (20α) dB/decade and phase remain constant at ($-90\alpha^{\circ}$). Additional flexibility can be provided by properties which allows the smooth adjustment of gain and phase characteristics in controller design.

Some fractional calculus applications require that the integral or derivative order is not maintained constant but is a function of a system parameter. VO derivative is the order of differentiation itself is a function or variable, it is achieved with VO differential equations and applies mostly to dynamical changing regime problems, such as variable viscoelasticity oscillators. In complex anomalous diffusion modelling the VO derivative model is used as an important tool [28, 29]. VO derivatives and VO-FC are widely used in different areas like in mechanics, applied to viscoelasticity, constitutive relationship, viscoelastic oscillator, modelling of transport processes, anomalous diffusion, control theory, ecological models, biological models, study random-order models, and so on. Various applications of VO derivative models have been reported in the literature [21-24, 30, 31].

The literature on VO derivatives and their applications mainly defines VO derivatives as a direct extension of the FO derivatives, replacing the constant FO derivative α , $\alpha \in \mathbb{R}^+$ by the time-varying function$\alpha(t)$: $[0, t], (0,1)$. However, as reported by [32], VO derivative and integral operators derived using straightforward extensions lack a rigorous mathematical framework. To be precise, the VO derivative and integral operators defined using this extension does not obey the fundamental theorem of calculus, that is, the VO derivative operator does not necessarily work as the left inverse of VO integral operator. An alternate and mathematically sound definition of VO derivatives and integrals based on the Scarpi derivatives is discussed in [32]. These Scarpi VO fractional derivative and integral operators obey the fundamental theorem of calculus and rely upon the Laplace domain representation of these FO operators [27-29] and Sonine conditions [30-38].

This study extends the results of [32] by analyzing non-Homogeneous linear VO systems, using Scarpi VO derivative definitions. The work, probably for the first ever time, reports the behavior of the linear VO systems for the change in the sinusoidal input frequency. It involves the numerical computation of frequency response analysis of linear VO systems. Frequency response analysis is particularly important for variable fractional-order systems (VFOSs) because their dynamics are more complex than those of classical integer-order systems and even constant fractional-order systems. It is shown –with extensive simulation studies that the parameters of the variable order affect the frequency-domain behavior of these systems. The salient contributions of this work can be summarized as:

1. Development of a systematic procedure for the frequency-domain analysis of linear variable-order (VO) systems.
2. Analysis of frequency response of the VO linear systems defined using Scarpi definition for a variety of variable-order functions.
3. Study of the effect of variable order function parameters on the frequency-domain behavior of VO systems.

The paper is organized as follows. Next section introduces the fundamentals of fractional calculus. VO frequency response and challenges are discussed in section 3. VO Scarpi differintegral operators are defined in section 4. Results are presented in section 5. Section 6 gives a detailed discussion on the results. The conclusion is given in section 7.

FRACTIONAL CALCULUS

Fractional calculus is the branch of mathematics with integrodifferential operators having arbitrary non-integer, real and complex orders. In recent years, researchers have been using this mathematical tool for modeling various real-world engineering complex systems. A good amount of theoretical research work on FC differential equations [39-41] has been carried out by researchers, and it is now well-developed. Nowadays, Fractional derivatives & integrals are used in many applications of science and engineering. The fundamental definitions of fractional derivatives are listed below:

A. Grunwald-Letnikov definition with derivative order $\alpha \in \mathbb{R}^+$. The fractional-order derivative is defined as

$$aD_t^{\alpha} f(t) = \lim_{h \to 0} h^{-\alpha} \sum_{j=0}^{\left[\frac{t-a}{h}\right]} (-1)^j \ {}^{\alpha}C_j f(t-jh) \tag{1}$$

where, $\left[\frac{t-a}{h}\right]$is the integer part of h and ${}^{\alpha}C_j$is the binomial coefficient.

B. Riemann-Liouville definition with derivative order $\alpha \in \mathbb{R}^+$: The fractional-order derivative is defined as

$$aD_t^{\alpha} f(t) = \frac{1}{\Gamma(n-\alpha)} \frac{d^n}{dt^n} \int_a^t \frac{f(\tau)}{(t-\tau)^{\alpha-n+1}} d\tau \tag{2}$$

for $n-1 < \alpha < n, \quad n \in \mathbb{Z}^+$ and $\Gamma(\cdot)$ is the Gamma function.

C. Caputo definition with derivative order $\alpha \in \mathbb{R}^+$: The fractional-order derivative is defined as

$$aD_t^{\alpha} f(t) = \frac{1}{\Gamma(n-\alpha)} \int_a^t \frac{f^n(\tau)}{(t-\tau)^{\alpha-n+1}} d\tau, \tag{3}$$

for $n-1 < \alpha < n, \quad n \in \mathbb{Z}^+$, where $f^n(\tau)$ is the derivative of n^{th}-order of function$f(t)$. The Caputo definition of a fractional derivative is most popular among researchers. To represent real-world systems in FO dynamics, fractional derivative (FD) definition in the Caputo sense has been used [15, 16]. For defining signals and functions in engineering systems, Caputo FD is commonly used. The FDE model with Caputo FD allows physical/measurable initial conditions. Numerous easy-to-simulate and implemented analytical and numerical methods are available to solve FDEs with Caputo FD [17]. The comparison of Caputo and analysis of variable-order fractional derivative algorithms is discussed in [18].

VO FREQUENCY RESPONSE AND CHALLENGES

For a standard fractional-order system, substituting $(s = j\omega)$ gives the frequency-dependent transfer function: $(G(j\omega) = \frac{1}{(j\omega)^{\alpha}+a})$. In a Variable Fractional-Order (VFO) system, the order depends on time or frequency, $(\alpha(t)) or (\alpha(\omega))$. Therefore, the frequency response is no longer a static transfer function; it becomes an evolving mathematical expression.

Frequency response analysis for variable-fractional-order linear systems (VFOLS) is difficult because there is no "constant" time-invariant transfer function due to the fact that the fractional order (α) changes with respect to time or state, thus the traditional Fourier and Laplace Transform techniques are not valid [13]. Consequently, VFOLS exhibit time dependent behavior, or iteration upon time/dependents of the system, that cannot be decoupled, therefore this is the primary challenge to performing frequency response analysis of VFOLs which creates several other analytical and mathematical challenges.

1. The presence of time-variant parameters in the system makes it impossible to represent it using a classic SMART algebraic transfer function, thus creating a breakdown in the original definition of an algebraic transfer function.
2. The principle of superposition and the principle of frequency invariance loss: In Linear Time-Invariant (LTI) systems, a sine wave input produces a sine wave output of identical frequency; however, in Variable-Frequency Operating Limit (VFOL) systems, these principles fail due to variable frequency inputs producing variable frequency outputs. The time variant nature of VFOL systems generates mixed frequencies and various harmonics, distorting the input/output relationship, thus nullifying the basic spectral mapping of linear systems.
3. Great computational complexity and numerical complexity: For solutions on the frequency response of VFOL systems, many times the time-varying orders can be converted into non-standard iterative scaling equations or non-standard approximations. There are rarely any analytical solutions available to researchers, few discussed in [19], which causes researchers to have to rely upon large numerical approximations that may yield results that have been mathematically unstable and that require excessive amounts of computational effort.
4. No standard criteria for determining stability: Since the characteristic equation of each VFOL system shifts dynamically, traditional frequency domain stability measures cannot be applied (e.g. Nyquist plots and Bode plots) to establish robustness with respect to bounded-input bounded-output (BIBO) stability; stable VFOL systems require the establishment of sophisticated and time-dependent envelopes rather giving traditional root finding methods.

SCARPI VO CALCULUS

This section presents the fundamental definitions of VO Scarpi derivatives and integral operators [32]. Consider an absolutely continuous function $f(t)$ defined in the interval $[0, T]$. As given in the previous section, the Caputo FD can be represented as follows:

$$ {}^{C}D_0^{\alpha} f(t) = \int_0^t \phi(t-\tau) f'(\tau)\, d\tau, \tag{4} $$

where the weakly-singular kernel is

$$ \phi(t) = \frac{t^{-\alpha}}{\Gamma(1-\alpha)}, \tag{5} $$

with $0 < \alpha < 1$

The Caputo FD of (4) acts as a left-inverse of the RL integral

$$ {}^{RL}I_0^{\alpha} f(t) = \int_0^t \psi(t-\tau)\, f(\tau)\, d\tau, \tag{6} $$

with the kernel

$$ \psi(t) = \frac{t^{\alpha-1}}{\Gamma(\alpha)} \tag{7} $$

The definitions (4) and (6) obey the fundamental theorem of calculus,

$$ {}^{C}D_0^{\alpha}\, {}^{RL}I_0^{\alpha} f(t) = f(t), $$

and

$$ {}^{\boldsymbol{RL}}\mathrm{I}_a^{c}\, {}^{c}\mathrm{D}_a \mathrm{f(t)} = \mathrm{f(t)} - \mathrm{f(0)} $$

The Laplace Transform (LT) of the kernels (5) and (7) are given as

$$ \phi(s) = \mathcal{L}\phi(t) = s^{\alpha-1}, \tag{8} $$

which can be rewritten as

$$ \phi(s) = s^{s\mathrm{A}(s)-1}, $$

Where

$$ \mathrm{A}(s) = \mathcal{L}\alpha(t) = \mathcal{L}\alpha = \frac{\alpha}{s}, \tag{9} $$

Similarly,

$$ \psi(s) = \mathcal{L}\psi(t) = \frac{1}{s^{\alpha}}, $$

which can also be represented as

$$ \psi(s) = s^{-s\mathrm{A}(s)}, \tag{10} $$

With $\mathrm{A}(s)$ as given in (9). With this, the Laplace transfer of Caputo FO derivative and integral operators (4) and (6) respectively can be established as:

$$ \mathcal{L}\{{}^{C}\mathrm{D}_0^{\alpha} f(t)\} = s^{s\mathrm{A}(s)} F(s) - s^{s\mathrm{A}(s)-1} f(0), \tag{11} $$

and

$$ \mathcal{L}\{{}^{RL}\mathrm{I}_0^{\alpha} f(t)\} = s^{-s\mathrm{A}(s)} F(s), \tag{12} $$

The above notions of FO operators can be extended to variable-order with the help of Laplace domain. Consider a locally integrable function $\alpha(t): [0, T] \to (0,1)$, with the Laplace transform

$$A(s) = \mathcal{L}(\alpha(t)) \tag{13}$$

The Scarpi VO derivative in the Caputo sense is defined by substituting (13) in (11) and the Scarpi VO integral operator is defined by substituting (13) in (12). Thus,

$$\mathcal{L}\{{}^{S}D_0^{\alpha(t)} f(t)\} = s^{sA(s)}F(s) - s^{sA(s)-1}f(0), \tag{14}$$

And

$$\mathcal{L}\{{}^{S}I_0^{\alpha(t)} f(t)\} = s^{-sA(s)}F(s), \tag{15}$$

As shown in [32], the VO operators defined in (14) and (15) satisfy the fundamental theorem of calculus, that is,

$${}^{S}D_0^{\alpha}(t)\, {}^{S}I_0^{\alpha}(t) f(t) = f(t)$$

And

$${}^{S}I^{\alpha(t)}\, {}^{S}D^{\alpha(t)} f(t) = f(t) - f(0)$$

The above identities hold if the two kernels $\phi_\alpha(t)$ and $\psi_\alpha(t)$ form a Sonine pair, that is

$$\int_0^t \phi_\alpha(t-\tau)\, \psi_\alpha(\tau) d\tau = 1, \quad t > 0 \tag{16}$$

which in Laplace domain is represented as

$$\phi_\alpha(s)\psi_\alpha(s) = \frac{1}{s}.$$

Further, as mentioned in [32], the Scarpi VO integral operator (15) is commutative and follows the semigroup property.

RESULTS

This section presents frequency-domain analysis and numerical analysis of linear VO systems with Scarpi definitions. This work considers VFO Non-Homogeneous linear system:

$${}^{S}D_0^{\alpha(t)} y(t) = -\lambda y(t) + u(t). \tag{17}$$

where, $\lambda > 0$ and $u(t)$ is the forcing function or input.

Following cases have been examined in this work.

Case	α(t)
Case 1	$\alpha(t) = \beta\, e^{-at}$
Case 2	$\alpha(t) = \beta\, e^{-at}\,(1 + \sin t)$
Case 3	$\alpha(t) = \alpha_2 + (\alpha_1 - \alpha_2)\, e^{-ct}$
Case 4	$\alpha(t) = \alpha_2 + (\alpha_1 - \alpha_2) E_\beta(-ct^\beta)$

Each VO system is simulated for the different cases, a detailed analysis is presented.

Consider the Non-Homogeneous VO fractional differential equation:

$$^{S}D_0^{\alpha(t)}y(t) = -\lambda y(t) + u(t),$$

where, $\lambda > 0$ and $u(t)$ is the forcing function (unit step) or input.

Solution for Non-Homogeneous VO fractional differential equation can be given as:

$$\mathcal{L}\{u(t)\} = U(s) = \frac{1}{(s^2+1)}, \tag{18}$$

where, $y(0) = y_0$, $\lambda > 0, \lambda \in R^+$

Laplace Transform of (18) gives $s^{sA(s)} + Y(s) - s^{sA(s)-1}y_0 + \lambda Y(s) = U(s)$

$$\left(s^{sA(s)} + \lambda\right)Y(s) = s^{sA(s)-1}y_0 + U(s)$$

$$Y(s) = \frac{U(s)}{(s^{sA(s)}+\lambda)} \tag{19}$$

To carry out the frequency domain response, Laplace domain s-plane to be converted to frequency domain $j\omega$ axis, involves substituting $s = j\omega$ (where $(\sigma = 0)$) into the transfer function, $(Y(s))$, to get $(Y(j\omega))$, which reveals the system's steady-state frequency domain response, effectively evaluating the system along the imaginary axis of the complex s-plane. This transformation focuses on purely oscillatory responses, removing the exponential growth/decay (damping) represented by the real part, (σ).

Substitute $s = j\omega$ in (19), which gives,

$$G(j\omega) = \frac{1}{(j\omega^{j\omega A j\omega)} + \lambda)} \tag{20}$$

Numerical analysis of linear VO system frequency response

Consider two complex numbers Z_1 and Z_2, $Z_1 = a + jb$ here magnitude is $r_1 e^{j\theta_1}$ angle is $r_1\angle\theta_1$. for second complex number, $Z_2 = c + jd$ here magnitude is $r_2 e^{j\theta_2}$ angle is $r_2\angle\theta_2$.

Let

$$M = Z_1^{Z_2},\ log_e M = Z_2\ log_e Z_1$$

$$log_e M = r_2\, e^{j\theta_2}\ log_e r_1\, e^{j\theta_1}$$

$$log_e M = r_2 e^{j\theta_2}[log_e r_1 + j\theta_1 log_e e]$$

$$log_e M = r_2 e^{j\theta_2}[log_e r_1 + j\theta_1] \tag{21}$$

$$M = e^{r_2\, e^{j\theta_2}\, [\,log_e r_1\, +\, j\, \theta_1\,]}$$

VO Linear System Simulation for Different Cases:

Case 1:

$$\alpha(t) = \beta e^{-at}, 0 < \beta < 1 \text{ and } a > 0.$$

Thus,

$$A(j\omega) = \frac{\beta}{j\omega + a}, \tag{22}$$

which gives

$$\psi_\alpha(j\omega) = j\omega^{\frac{-\beta j\omega}{j\omega+a}}, \tag{23}$$

$$G(s) = \frac{1}{s^{\frac{-\beta s}{s+a}}+\lambda} \tag{24}$$

$$G(j\omega) = \frac{1}{j\omega^{\frac{-\beta j\omega}{j\omega+a}}+\lambda}$$

This is of the form, $j\omega^{\frac{-j\beta\omega}{j\omega+a}} = Z_1^{Z_2}$ where, $Z_1 = j\omega$, and $Z_2 = \frac{-j\,\beta\,\omega}{j\omega + a}$.

Rearrange for Z_2,

$$Z_2 = \frac{-j\beta\omega}{j\omega+a} * \frac{a-j\omega}{a-j\omega}\text{ , after solving, } Z_2 = \frac{-\beta\omega^2-j\beta a\omega}{a^2+\omega^2}$$

$$Z_2 = \frac{-\beta\omega^2}{a^2+\omega^2} - j\,\frac{\beta a\omega}{a^2+\omega^2} \tag{25}$$

Assuming equation in generalized form as $Z_2 = A + jB$,

Again, $Z_1 = j\omega = \omega\, e^{j\frac{\pi}{2}} = \omega\, e^{j\frac{\pi}{2}}$ and $r_1 = \omega, and\ \theta_1 = \frac{\pi}{2}$

Similarly, for Z_2, magnitude is $r_2 = \sqrt{A^2 + B^2}$ phase angle $\theta_2 = tan^{-1}\left(\frac{B}{A}\right)$

referring to equation (21)

$$M = exp\left[(c + j\,d)\left(log_e^{r_1} + j\,\theta_1\right)\right]$$

$$M = exp[(clog_e r_1 - d\theta_1)] + exp[j(dlog_e r_1 + c\theta_1)]$$

$$M = exp[(clog_e r_1 - d\theta_1)] + [\cos(dlog_e r_1 + c\theta_1) + j\sin(dlog_e r_1 + c\theta_1)] \tag{26}$$

so, $G(j\omega) = \frac{1}{M+\lambda}$

consider, $M = M_1[\cos M_2 + j\sin M\,3]$

we get,

$$Y(j\omega) = \frac{1}{((j\omega)^2+1)\left(j\omega^{\left(\frac{-j\omega\beta}{j\omega+a}\right)}+\lambda\right)} \tag{27}$$

The response is observed by variations in the parameters, like for fixed value of $\lambda = 1$, keep β constant as $\beta = 0.95$ and $a = 10$. The frequency response/ Bode plot of $y(t)$ is as shown in figure (1).

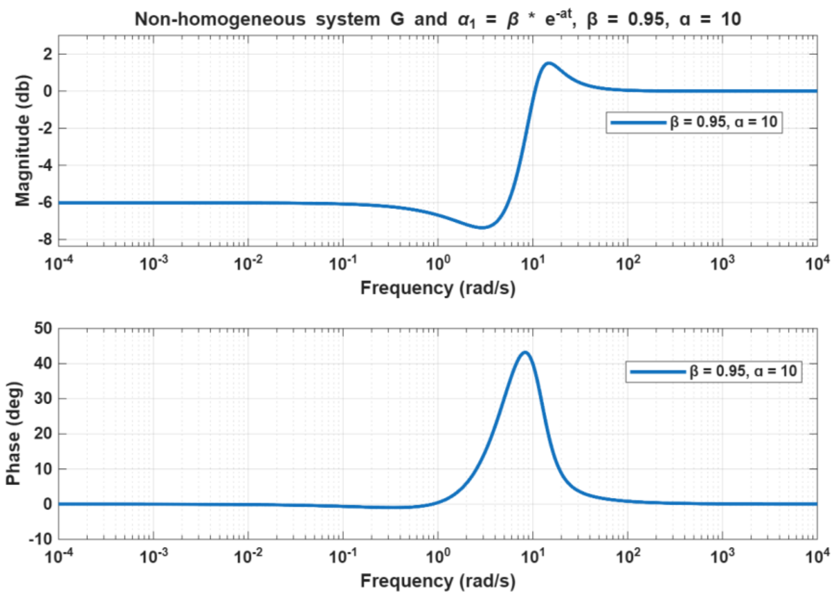

<u>Figure 1</u>: Frequency response of Non-Homogeneous VOFDE G, $\alpha(t) = \beta e^{-at}$ with $a = 10, \beta = 0.95$ and $\lambda = 1$

Following observations are noted for frequency response:

1. For frequencies from $\omega = 10^{-4\ \text{rad/s}}$ up to approximately $10^{-1\ \text{rad/s}}$, the system magnitude is completely flat at -6 dB (corresponding to a linear gain of 0.5). At the same time, the phase response steady at $0°$, which represents low-frequency steady-state regime.
2. Between $\omega = 10^{-1\ \text{rad/s}}$ and 3 rad/s, the magnitude undergoes towards a localized minimum of roughly $-7.4\ dB, \omega = 2.5$ rad/s, also, the phase exhibits a minimal negative deviation before sharply reversing upward.
3. A rapid rise in magnitude can be observed within the $\omega = 3$ rad/s to 30 rad/s transition band. The system experiences peaking at approximately +1.5 dB $\omega \approx 15$ rad/s which is resonant peak. Phase lead dynamics are paired with a prominent phase lead peak reaching $+44°$ cantered tightly around $\omega \approx 8$ rad/s.
4. For all frequencies above $\omega = 10^{2\ rad/s}$, the magnitude response levels out precisely at 0 dB (unity gain), while the phase asymptotes back to $0°$.

Here, frequency-dependent variable exponent $j\omega A(j\omega)$ creates a highly localized structural transition. The exponential rate parameter $a = 10$ defines the critical dynamic boundary of the system's memory effect. The shift from a low-frequency gain to a high-frequency gain of alongside a positive phase side indicates that the Scarpi variable-order derivative inherently introduces a lead-network/high-pass shelving characteristic. The sharp phase peaks in the plot indicates that changing the functional form of the variable-order derivative allows for highly customizable frequency-shaping capabilities.

To confirm that the physical resonance of the variable-order system G, which is correlated with the generalized frequency response, physically exists, a harmonic excitation at the peak frequency (14.81 rad/s) was used to excite the system per the predictions from the Bode plot in Figure 1. In this case, the system is maximumly transmitting when the time-variable derivative order is determined by $\alpha_1 = \beta e^{-at}$, which is defined as the maximum value of α. Table 2 shows time-domain tracking of the various parameter configurations of β and a, with the representative resonant trajectories in figure 2.

Table 2: Maximum gain values at different angular frequencies for variation in a value.

a	ω	$M\ (G_{max})$
10	14.81	1.5091
100	78.0510	3.3713
1000	526.4344	5.1093760

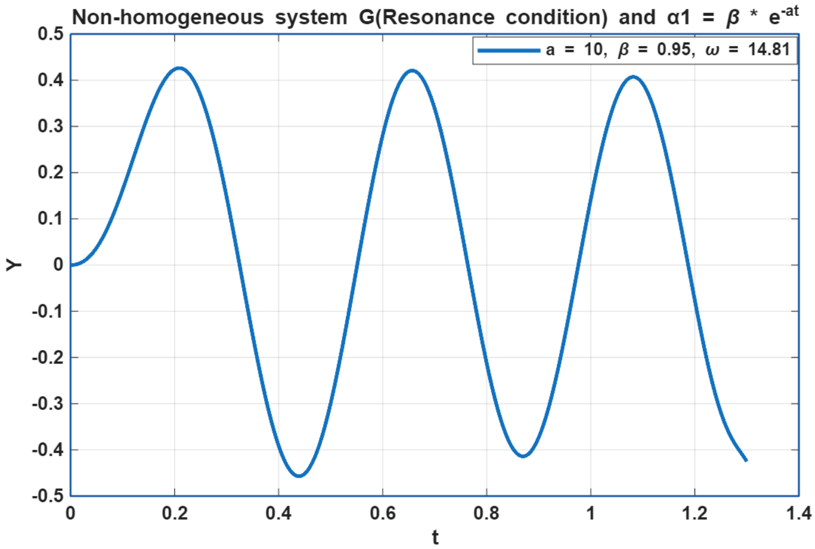

Figure 2: Resonance condition of Frequency response of Non-Homogeneous VOFDE G, $\alpha(t) = \beta e^{-at}$

Resonance Condition:

The system responds smoothly at first and has a zero slope from the start of response as well. There is an obvious asymmetry in the transient overshoot in the first cycle, which decreases with time; fully transitioned to a steady-state sinusoidal oscillation at the end of three full cycles (approximated to occur within 1.27 seconds) and with a calculated period equal to $\omega = \frac{2\pi}{T} \approx \frac{2\pi}{0.424} \approx 14.82\ \mathrm{rad/s}$. The mathematically calculated frequency identifies with the resonant frequency observed as a peak in the Bode plots at ω = 14.81 rad/s. The system produces a steady-state output of continuous high magnitude which supports that the model accurately represents the physical characteristics of a variable order system. Applications for this would include viscoelastic damping and living tissue where the effects of memory are short-lived when cyclically damaged. The results of this plot show that to model a material or component according to Scarpi's model, one could expect them to experience an initial period of adjustment, and after which, provide a predictable stable oscillatory path under continuous resonant loads.

Case 2

When

$$\alpha(t) = \beta e^{-at}(1+\sin t), \beta \in (0,0.5)\ a \in R^{+}$$

$$A(j\omega) = \beta\left[\frac{1}{j\omega+a} + \frac{1}{(j\omega+a)^2+1}\right] \quad (28)$$

$$\psi_\alpha(j\omega) = -\beta j\omega\left[\frac{1}{j\omega+a} + \frac{1}{(j\omega+a)^2+1}\right] \quad (29)$$

Substituting these values of $A(j\omega)$ and $\psi_\alpha A(j\omega)$ in equation (20), the frequency response of G to initial condition $y_0 = 0$ $U(j\omega) = \frac{1}{j\omega}$. The values of β and a considered in the analysis.

Here, by considering a value of $\lambda = 1, a = 1$ and $\beta = 0.95$, the frequency response of $y(t)$ obtained as shown in figure 3.

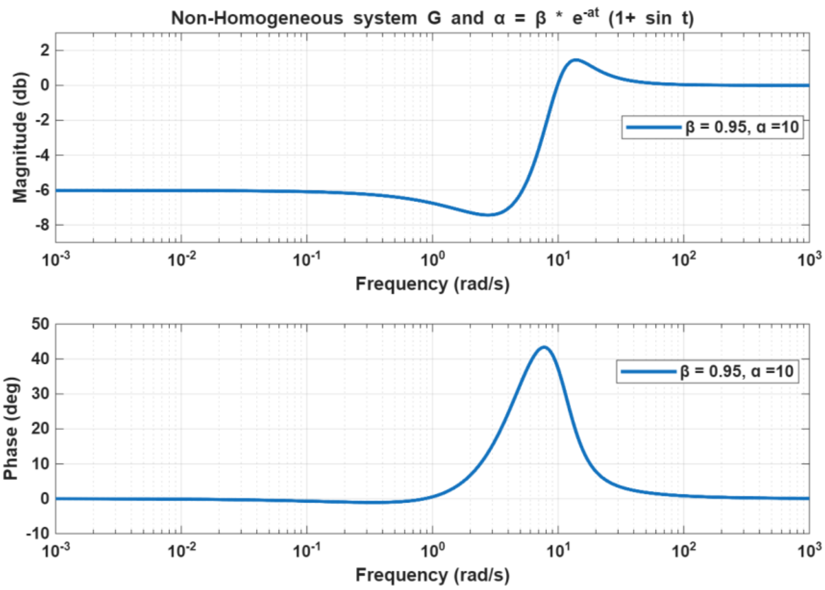

Figure 3: Frequency response of Non-Homogeneous VOFDE G, $\alpha(t) = \beta e^{-at}(1+\sin t)$ with $a = 10$, $\beta = 0.95$ and $\lambda = 1$.

From the response it has been observed that:

The magnitude response remains perfectly flat at -6 dB, and the phase response is locked exactly at $0°$. Between $\omega = 10^{-1\ \text{rad/s}}$ and 3 rad/s, response reaches a local minimum and the phase drops slightly below $0°$. In the 3 to 30 rad/s band, the system shows a sharp resonance behavior. The magnitude rises rapidly to a peak of +1.5 dB. Beyond $\omega = 10^{2\ \text{rad/s}}$, the magnitude settles back to 0 dB (unity gain), and the phase returns asymptotically to $0°$.

From above observations we can conclude: With the inclusion of term $(1+\sin t)$, periodic, time-varying modulation is introduced to the system's memory profile. This indicates that the Scarpi frequency-domain framework successfully captures time-averaged spectral energy transfer of the system and filter out the fluctuations and provide a robustness to a system.

Case 3

$$\alpha(t) = \alpha_2 + (\alpha_1 - \alpha_2)e^{-ct}$$

For $0 < \alpha_1 < \alpha_2 < 1$ and a real constant $c > 0$, we consider the function with

$$\psi_\alpha(j\omega) = j\omega^{-\frac{\alpha_2 c + \alpha_1 j\omega}{j\omega(j\omega + c)}} \tag{30}$$

we have,

$$\mathrm{A}(j\omega) = \frac{\alpha_2 c + \alpha_1 j\omega}{j\omega(j\omega + c)} \tag{31}$$

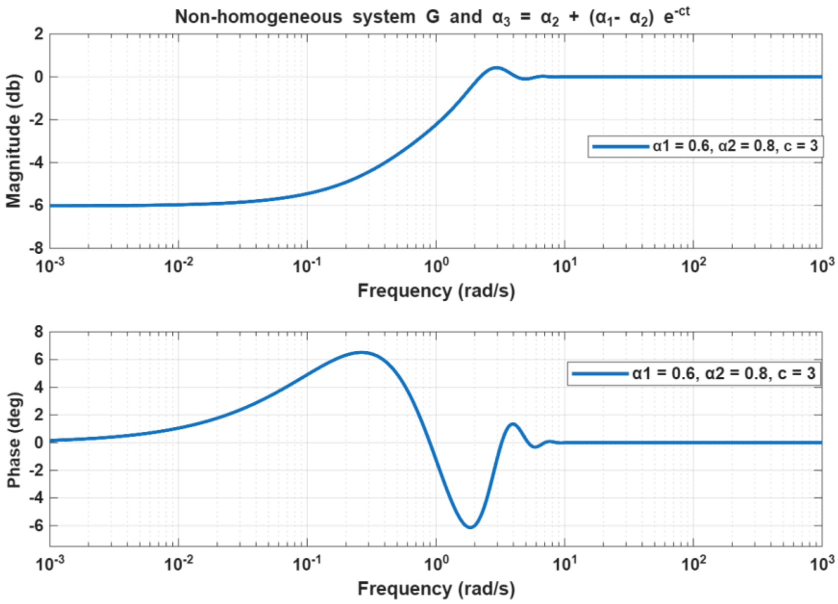

Figure 4: frequency response for initial condition y_0 for Non-Homogeneous VOFDE G, $\alpha(t) = \alpha_2 + (\alpha_1 - \alpha_2)e^{-ct}$, with constant $\alpha_1 = 0.6$, $\alpha_2 = 0.8$ and vary $c = 3$ and $\lambda = 1$.

We considered some variations in the parameters, the value of $\lambda = 1$, $\alpha_1 = 0.6$, $\alpha_2 = 0.8$, $\beta = 0.1$ and $c = 3$. The frequency response of $y(t)$ is as shown in figure 4. Some of the observations are given below:

In this case the magnitude response has a much steeper slope and continues to incline sooner than typically expected. The phase response displays an unusually complex multi-modal behavior in the mid-frequency band. This plot also clearly demonstrates the workings of an order-switching system in the frequency domain. The detection of these alternating phase behaviors serves as an unmistakable means of identifying papers with their focus on variable order fractional differential equations (VOFDE). If the experimental system such as an electrochemical battery or viscoelastic damper exhibits this type of localized phase behavior through the course of the experiment, it provides a very strong indication that the underlying physical process is experiencing a transition through a nonstationary memory characterized by a bounded order switching operator.

Case 4

The above cases can be represented in a general way by replacing the exponential with the Mittag-Leffler function, given as similar to a homogeneous system.

$$\alpha(t) = \alpha_2 + (\alpha_1 - \alpha_2)E_\beta\left(-ct^\beta\right)$$

$$A(j\omega) = \frac{\alpha_1 j\omega^\beta + \alpha_2 c}{j\omega\left(j\omega^\beta + c\right)} \quad (32)$$

$$\psi_\alpha(j\omega) = j\omega^{-\frac{\alpha_1 j\omega^\beta + \alpha_2 c}{j\omega\left(j\omega^\beta + c\right)}} \quad (33)$$

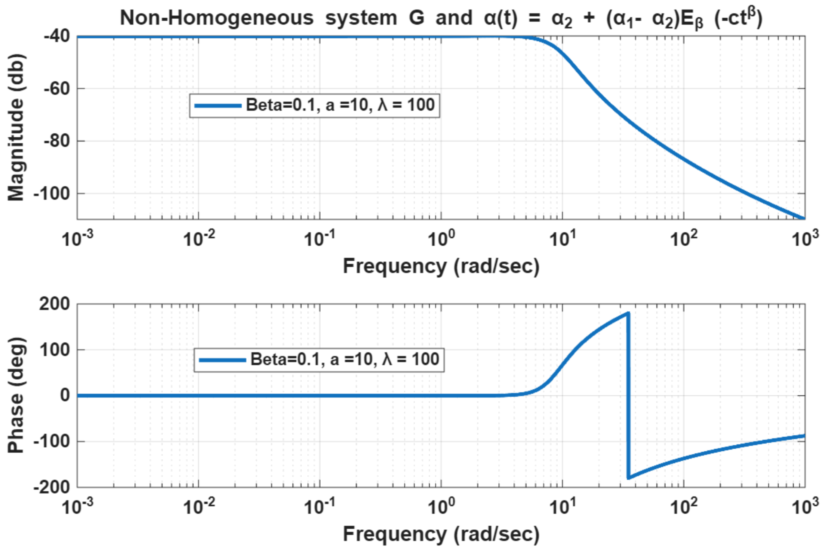

Figure 5: Frequency response with time for initial condition y_0 for Non-Homogeneous VOFDE G, $\alpha(t) = \alpha_2 + (\alpha_1 - \alpha_2)E_\beta\left(-ct^\beta\right)$, with constant $\alpha_1, \alpha_2, c = 3, \beta = 0.1$ and $\lambda = 100$.

We considered some variations in the parameters, the value of $\lambda = 100, \alpha_1 = 0.6, \alpha_2 = 0.8, \beta = 0.1$ and c = 3. The frequency response of $y(t)$ is as shown in figure 5. Some observations are noted as follows:

The frequency response is essentially flat at a very low (-40 dB) level; meanwhile, the phase response remains fixed at 0°. This combination of parameters effectively turns the VOFDFE into a typical and very robust low pass filter. In addition, because the large value of the parameter, λ = 100, dominates the denominator of the generalized system, G(jω), so that the low frequency gain must be -40dB, causes the memory order of the Mittag-Leffler function transitions between β = 0.1, which demonstrates that this is a very slow, long memory (heavy tail) time domain relaxation process, rather than a fast/standard exponential decay. In the frequency domain; this long memory and slow behaviour will cause a continuous phase accumulation across a narrow frequency range $(0^\circ \rightarrow 180^\circ)$ indicating there are extremely anomalous material and/or medium energy storage characteristics within that volume of material. The rapid increase in phase to 180° is going to create a critical phase inversion in the system at the frequency of ω = 33 radians/second. Any negative feedback loop that crosses in proximity to this frequency will automatically toggle to positive feedback, and cause an extreme closed-loop instability.

DISCUSSION

The previous study explores the distinct frequency response characteristics of a non-homogeneous linear system; this study focused on four different functional cases of fractional-order variable ($\alpha(t)$). All four cases support the concept that the frequency response will change with the structural nature of $\alpha(t)$ (which represents either time or space as the independent variable); thus, as $\alpha(t)$ changes, the frequency response will impact the system's phase, filtering and resonant characteristics.

The characteristics of Cases 1 and 2 are very similar, exhibiting characteristics of high-pass/notch-type filtering at the high end of the frequency response and -6 dB magnitude stability in the low-frequency region of the magnitude plot. Both Cases 1 and 2 also have similarly noticeable positive phase lead peaks. The second case's periodic sinusoidal perturbation does not introduce any significant distortion to the steady-state Bode magnitude or phase envelope.

The high-pass/notch filtering characteristic observed in case 3 is the result of an overall smooth transition function; therefore, in case 3, the notch type behavior has been completely removed and the system acts as a completely smooth high-pass filter.

In contrast to Cases 1 and 2, the Mittag-Leffler-driven order in Case 4 results in a complete inversion of the characteristic topology, thereby creating a heavily attenuated low-pass filter characteristic and providing proof that non-local memory profile characteristics will have a drastically different impact on energy transmission through this system.

Generally, in a traditional linear time invariant (LTI) systems, resonance is determined by fixed pole and zero locations. However, in this variable fractional-order systems, Non-homogeneous systems the peak resonance location is determined very much by the mathematical trajectory of α(t). Case 1 and Case 2 demonstrate a unique notch peak hybrid resonance. Case 3 demonstrates how the order transition profile has become smoothed and is merely an indication of an active damper affecting the resonant modes of the system. In Case 4- Mittag-Leffler profile, the phenomenon of resonance has completely been removed from the magnitude plot and has been replaced with smooth, monotonically low pass roll-off.

CONCLUSION

Application of the variable fractional-order non-homogeneous system G presents significant functional versatility, leading to the conclusion that the classifications associated with the fundamental filtering characteristics of the system are not stationary and will change dynamically with respect to the profile of $\alpha(t)$. Exponential or periodic profile(s): In both cases 1 and 2, the performance of the applications would be optimally achieved when expediting mid-band phase lead compensation and providing high-pass filtering with low frequency attenuation to a fixed constraint. Smooth transition profile: Applications requiring high-pass transition from low to high frequency via smooth, monotonic transitions are well suited to performance avoidance of mid-band notch dips as discussed for case 3. Mittag-Leffler memory profile, case 4: Will dramatically change the system from a high-attenuation-low-pass-filter to a high-pass-filter with extreme high frequency phase shifts. These results provide evidence that changing the fractional-order parameter dynamically provides a powerful synthesis tool that will allow a single non-homogeneous system architecture to transition from high-pass, notch-resonant, or low-pass with very high levels of attenuation simply through modulation of the fractional-order control law.

REFERENCES

[1] I. Podlubny, “Fractional-order systems and PIRDμ-controllers,” IEEE Transactions on Automatic Control, vol. 44, no. 1, pp. 208–214, 1999.

[2] I. Batiha, M. S. Alshorm, I. Jebril, and M. A. Hammad, “A brief review about fractional calculus,” International Journal of Open Problems in Computer Mathematics, vol. 15, no. 4, 2022.

[3] Z. Li, L. Liu, S. Dehghan, Y. Chen, and D. Xue, “A review and evaluation of numerical tools for fractional calculus and fractional order controls,” International Journal of Control, vol. 90, no. 6, pp. 1165–1181, 2017.

[4] C. A. Monje, Y. Chen, B. M. Vinagre, D. Xue, and V. Feliu-Batlle, Fractional-Order Systems and Controls: Fundamentals and Applications. Springer Science & Business Media, 2010.

[5] Chyi Hwang,Jeng-Fan Leu,and Sun-Yuan Tsay,“A Note on Time-Domain Simulation of Feedback Fractional-Order Systems”, IEEE Trans. Automat. Contr., Vol.47, pp.625 – 631, 2002.

[6] H. Sun, Y. Zhang, D. Baleanu, W. Chen, and Y. Chen, “A new collection of real-world applications of fractional calculus in science and engineering,” Communications in Nonlinear Science and Numerical Simulation, vol. 64, pp. 213–231, 2018.

[7] Y. Wei, Q. Gao, C. Peng, and Y. Wang, “A rational approximate method to fractional order systems,” International Journal of Control, Automation and Systems, vol. 12, no. 6, pp. 1180–1186, 2014.

[8] J. S. Naick, G. C. Sekhar, N. C. Kotaiah, M. Anitha, and B. G. R. Naik, “Optimizing solar and wind energy integration in grid-connected EV fast charging systems using fuzzy logic control for improved stability and power quality,” SSRG International Journal of Electrical and Electronics Engineering, vol. 11, no. 12, pp. 119–136, 2024.

[9] Radwan, A.G. and Salama, K.N., 2012. Fractional-order RC and RL circuits,” Circuits, Systems, and Signal Processing, 31(6), pp.1901-1915, 2012.

[10] M. A. Pakzad, S. Pakzad, and M. A. Nekoui, “Stability analysis of time-delayed linear fractional-order systems,” International Journal of Control, Automation and Systems, vol. 11, pp. 519–525, 2013.

[11] S.D. Lin, C.H. Lu, Laplace transform for solving some families of fractional differential equations and its applications. *Adv. Difference Equ.* **2013**, No 1 (2013), 137.

[12] Q. Liu and S. Tian, “Iterative learning control analysis for linear fractional-order singular systems,” International Journal of Control, Automation and Systems, vol. 20, no. 12, pp. 3951–3959, 2022.

[13] A. Charef and H. Nezzari, “On the fundamental linear fractional order differential equation,” Nonlinear Dynamics, vol. 65, no. 3, pp. 335–348, 2011.

[14] Jifeng, W. and Yuankai, L., 2005, January. Frequency domain analysis and applications for fractional-order control systems. In Journal of physics: Conference series (Vol. 13, No. 1, pp. 268-273).

[15] B. Ross, Ed., Fractional Calculus and Its Applications: Proceedings of the International Conference Held at the University of New Haven. USA: Springer, 1975.

[16] A. A. Kilbas, H. M. Srivastava, and J. J. Trujillo, Theory and Applications of Fractional Differential Equations, vol. 204. Elsevier, 2006.

[17] A. Atangana, “Fractional operators and their applications,” in Fractional Operators with Constant and Variable Order with Application to Geo-Hydrology. Netherlands: Academic Press, pp. 79–112, 2018.

[18] D. Amilo, K. Sadri, and E. Hincal, “Comparative analysis of Caputo and variable-order fractional derivative algorithms across various applications,” International Journal of Applied and Computational Mathematics, vol. 11, no. 3, p. 80, 2025.

[19] Valério, D. and Da Costa, J.S., 2011. Variable-order fractional derivatives and their numerical approximations. Signal processing, 91(3), pp.470-483.

[20] Allogmany, R., Almuallem, N.A., Alsemiry, R.D. and Abdoon, M.A., 2025. Exploring chaos in fractional order systems: A study of constant and variable-order dynamics. Symmetry, 17(4), p.605.

[21] Sun, H., Chang, A., Zhang, Y. and Chen, W., 2019. A review on variable-order fractional differential equations: mathematical foundations, physical models, numerical methods and applications. Fractional calculus and applied analysis, 22(1), pp.27-59.

[22] Caponetto, R., Dongola, G., Fortuna, L. and Petras, I., 2010. Fractional order systems: modeling and control applications (Vol. 72). World scientific.

[23] Wang, Y., Li, J., Qin, Y., Fan, L., Liu, X., Song, Y. and Han, W., 2025. Analysis of the characteristics of variable-order fractional viscoelastic oscillator under impact loading. International Journal of Non-Linear Mechanics, p.105206.

[24] Naveen, S. and Parthiban, V., 2024. Qualitative analysis of variable-order fractional differential equations with constant delay. Mathematical Methods in the Applied Sciences, 47(4), pp.2981-2992.

[25] C. Srisailam and M. Manjula, “Optimized FOPID controller for transient stability improvement in a microgrid with energy storage,” SSRG International Journal of Electrical and Electronics Engineering, vol. 10, no. 2, pp. 19–34, 2023.

[26] C. A. Monje, B. M. Vinagre, V. Feliu, and Y. Chen, “Tuning and auto-tuning of fractional order controllers for industry applications,” Control Engineering Practice, vol. 16, no. 7, pp. 798–812, 2008.

[27] H. Sun, A. Chang, Y. Zhang, and W. Chen, “A review on variable-order fractional differential equations: Mathematical foundations, physical models, numerical methods and applications,” Fractional Calculus and Applied Analysis, vol. 22, no. 1, pp. 27–59, 2019.

[28] S. Sarwar, "On the existence and stability of variable order Caputo type fractional differential equations," Fractal and Fractional, vol. 6, no. 2, p. 51, 2022.

[29] S. G. Samko, "Fractional integration and differentiation of variable-order," Analysis Mathematica, vol. 21, no. 3, pp. 213–236, 1995.

[30] S. Patnaik, J. P. Hollkamp, and F. Semperlotti, "Applications of variable-order fractional operators: A review," Proceedings of the Royal Society A, vol. 476, no. 2234, p. 20190498, 2020.

[31] M. D. Ortigueira, D. Val´erio, and J. T. Machado, "Variable order fractional systems," Communications in Nonlinear Science and Numerical Simulation, vol. 71, pp. 231–243, 2019.

[32] R. Garrappa, A. Giusti, and F. Mainardi, "Variable-order fractional calculus: A change of perspective," Communications in Nonlinear Science and Numerical Simulation, vol. 102, p. 105904, 2021.

[33] R. T. Sibatov, P. E. L'vov, and H. Sun, "Variable-order fractional diffusion: Physical interpretation and simulation within the multiple trapping model," Applied Mathematics and Computation, vol. 482, p. 128960, 2024.

[34] R. Garrappa, A. Giusti, and F. Mainardi, "Variable-order fractional calculus: From old to new approaches," in Proc. Int. Conf. Fractional Differentiation and Its Applications (ICFDA), pp. 1–6, 2023.

[35] G. Fern´andez-Anaya, F. A. God´ınez, R. Vald´es, L. A. Quezada-T´ellez, and M. A. Polo-Labarrios, "A simple fractional model with unusual dynamics in the derivative order," Fractal and Fractional, vol. 9, p. 264, 2025.

[36] A. Giusti, I. Colombaro, R. Garra, R. Garrappa, and A. Mentrelli, "On variable-order fractional linear viscoelasticity," Fractional Calculus and Applied Analysis, vol. 27, no. 4, pp. 1564–1578, 2024.

[37] A. Stanislavsky and A. Weron, "Duality of fractional systems," Communications in Nonlinear Science and Numerical Simulation, vol. 101, p. 105861, 2021.

[38] Y. Luchko, "General fractional integrals and derivatives with the Sonine kernels," Mathematics, vol. 9, no. 6, p. 594, 2021.

[39] M. R. Ali, U. Ghosh, S. Sarkar, and S. Das, "Analytic solution of the fractional-order non-linear Schr¨odinger equation and the fractional-order Klein–Gordon equation," Differential Equations and Dynamical Systems, vol. 30, pp. 499–512, 2022.

[40] S. Shahmorad, S. Pashayi, and M. S. Hashemi, "Numerical solution of a nonlinear fractional integro-differential equation by a geometric approach," Differential Equations and Dynamical Systems, vol. 29, pp. 585–596, 2021.

[41] B. T. Krishna, "Studies on fractional-order differentiators and integrators: A survey," Signal Processing, vol. 91, no. 3, pp. 386–426, 2011.